JOURNAL OF VIROLOGY, May 2007, p. 4501–4509 Vol. 81, No. 9
0022-538X/07/$08.00+0 doi:10.1128/JVI.02719-06

Switching the Substrate Specificity of the Two-Component NS2B-NS3 Flavivirus Proteinase by Structure-Based Mutagenesis▽

Sergey A. Shiryaev,[1] Boris I. Ratnikov,[1] Alexander E. Aleshin,[1] Igor A. Kozlov,[2] Nicholas A. Nelson,[2] Michal Lebl,[2] Jeffrey W. Smith,[1] Robert C. Liddington,[1] and Alex Y. Strongin[1]*

Burnham Institute for Medical Research, La Jolla, California,[1] and Illumina, Inc., San Diego, California[2]

Received 9 December 2006/Accepted 19 January 2007

The flavivirus NS2B-NS3(pro)teinase is an essential element in the proteolytic processing of the viral precursor polyprotein and therefore a potential drug target. Recently, crystal structures and substrate preferences of NS2B-NS3pro from Dengue and West Nile viruses (DV and WNV) were determined. We established that the presence of Gly-Gly at the P1′-P2′ positions is optimal for cleavage by WNV NS3pro, whereas DV NS3pro tolerates well the presence of bulky residues at either P1′ or P2′. Structure-based modeling suggests that Arg^{76} and Pro^{131}-Thr^{132} limit the P1′-P2′ subsites and restrict the cleavage preferences of the WNV enzyme. In turn, Leu^{76} and Lys^{131}-Pro^{132} widen the specificity of DV NS3pro. Guided by these structural models, we expressed and purified mutant WNV NS2B-NS3pro and evaluated cleavage preferences by using positional scanning of the substrate peptides in which the P4-P1 and the P3′-P4′ positions were fixed and the P1′ and P2′ positions were each randomized. We established that WNV R76L and P131K-T132P mutants acquired DV-like cleavage preferences, whereas T52V had no significant effect. Our work is the first instance of engineering a viral proteinase with switched cleavage preferences and should provide valuable data for the design of optimized substrates and substrate-based selective inhibitors of flaviviral proteinases.

Dengue and West Nile viruses (DV and WNV) are members of the flavivirus genus within the *Flaviviridae* family. Four distinct, but structurally similar, serotypes represent DV (13). Flaviviruses are transmitted to animals, including humans, by either mosquito or tick bites. Flaviviruses are encoded by a single-strand, positive-sense, 11-kb RNA genome, which serves as an mRNA for protein synthesis and as a template for RNA replication in the host cell. There are three structural proteins (C, prM, and E) and seven nonstructural proteins (NS1, NS2A, NS2B, NS3, NS4A, NS4B, and NS5) encoded by the viral genome (21). Proteinases of the host (furin and secretase) and of the virus [NS3 serine (pro)teinase (NS3pro)] are required for the complete processing of the polyprotein precursor and its transformation into mature viral proteins (4, 27, 31, 34). Full-length NS3 is a bifunctional protein: its N-terminal and C-terminal portions encode the NS3pro domain and the helicase (NS3hel) domain, respectively (33, 35). NS3pro is responsible for cleavage of the capsid protein C, as well as the boundaries between NS2A/NS2B, NS2B/NS3, NS3/NS4A, NS4A/NS4B, and NS4B/NS5 (6, 24).

NS2B is an essential cofactor of NS3pro, and it is located immediately upstream in the polyprotein precursor (5, 9, 25, 26). The NS2B sequence includes three to four transmembrane helices that anchor the NS2B-NS3 heterodimer to the endoplasmic reticulum membrane. In vitro, the cofactor activity of the 35- to 48-residue central portion of NS2B is approximately equivalent to that of the entire NS2B sequence (11, 12, 19). Mutations in the NS3pro cleavage motifs in the polyprotein precursor abolish viral infectivity (2). These characteristics make NS3pro a promising and attractive target for flaviviral drugs.

Recently, the crystal structures of DV and WNV NS2B-NS3pro, as well as the cofactor-free NS3pro, have been determined (1, 10, 22, 23). These structures reveal a novel mechanism of cofactor-induced proteinase activation, in which NS2B induces a rearrangement of the NS3pro global fold and directly contributes to the architecture and specificity of the active site.

Significant interactions of NS2B-NS3pro with its cleavage motifs appear to be restricted to the P2-P2′ sites (20, 29, 30, 36). Our substrate profiling study determined that the WNV proteinase was highly selective and that the motif (K/R)(K/R) ↓ GG was optimal for cleavage. In contrast, DV proteinase was less selective and tolerated well the presence of bulky Trp, Phe, or Tyr at either the P1′ or the P2′ site, provided the other position was occupied by Gly. The distinct preferences of the two proteinases allowed us to design peptide substrates that were selectively cleaved by DV and WNV NS3pro (20, 26, 29, 30).

To extend our understanding of the structural parameters that define flaviviral proteinase specificity, we used structure-guided mutagenesis to alter the substrate preference of WNV NS3pro. We describe here mutations that transform the WNV NS3pro into a proteinase with DV cleavage preferences. The results validate the structure of the DV and WNV NS2B-NS3pro and contribute to our understanding of their roles in the flavivirus life cycle. These results also provide a biochemical resource to expedite structure-based design of novel and specific inhibitors of flavivirus proteinases.

MATERIALS AND METHODS

Reagents. Reagents were purchased from Sigma-Aldrich (Milwaukee, WI) unless indicated otherwise. Solvents for peptide synthesis were obtained from VWR (West Chester, PA). Fmoc (9-fluorenylmethoxy carbonyl) amino acids, benzotriazole-1-yl-oxy-tris-(dimethylamino)-phosphoniumhexafluorophosphate (BOP reagent), and biotin resin were purchased from EMD Biosciences (San

* Corresponding author. Mailing address: The Burnham Institute, 10901 North Torrey Pines Road, La Jolla, CA. Phone: (858) 713-6271. Fax: (858) 713-9925. E-mail: strongin@burnham.org.

▽ Published ahead of print on 14 February 2007.

Diego, CA). Pyroglutamic acid-RTKR-7-amino-4-methylcoumarin (Pyr-RTKR-AMC) was purchased from American Peptide (Sunnyvale, CA).

Enzyme cloning, expression, and purification. Cloning of the wild-type NS2B-NS3 proteinases from DV and WNV was reported earlier (29, 30). The 48-residue central portion of NS2B was linked to the NS3pro sequence via GGG GSGGGG (WNV) and GGGGSGGQQ (DV) linkers. The linker sequence was insignificantly modified in the DV construct to improve the crystallization properties of the protein. The T52V NS2B-NS3 mutant was prepared by PCR mutagenesis with 5′-GGTGTTTTCCACGTCCTTTGGCATACAACA-3′ and 5′-TGTTGTATGCCAAAGGACGTGGAAAACACC-3′ forward and reverse primers, respectively (the mutant nucleotides are underlined) and with the wild-type NS2B-NS3pro cDNA template. 5′-GTCAAGGAGGATCTACTTTG TTACGGAGGA-3′ and 5′-TCCTCCGTAACAAAGTAGATCCTCCTTGA C-3′ forward and reverse primers were used to generate the R76L mutant. The P131K-T132P NS2B-NS3pro mutant was prepared with 5′-GGGGCCGTGAC TTTGGACTTCAAACCTGGAACATCAGGCTCACC-3′ and 5′-GGTGAGC CTGATGTTCCAGGTTTGAAGTCCAAAGTCACGGCCCC-3′ forward and reverse primers.

After we confirmed their authenticity by sequencing, the constructs were recloned into pET101 expression vectors. Competent *Escherichia coli* BL21(DE3) Codon Plus cells (Stratagene, San Diego, CA) were transformed with recombinant pET101 vectors. Transformed cells were grown at 30°C in Luria-Bertani broth containing ampicillin (0.1 mg/ml). Cultures were induced with 0.6 mM IPTG (isopropyl-β-D-thiogalactopyranoside) for 16 h at 18°C. The NS2B-NS3pro constructs, C terminally His_6 tagged, were purified from the supernatant fraction on a Co^{2+}-chelating Sepharose FastFlow column (30).

Peptide synthesis and cleavage. The design of a centrifugation-based, parallel peptide synthesizer, the techniques for purification and characterization of the peptides, and the control and cleavage reaction parameters were all described in detail previously (14, 16–18, 29). Briefly, peptide synthesis was performed in wells of a 96-well flat bottom polypropylene microtiter plate (Evergreen Scientific, Los Angeles, CA). Peptides exhibited 6(5)-carboxyfluorescein (FAM) and Gly-biotin at the N and C termini, respectively. Peptide purity was confirmed by reversed-phase high-pressure liquid chromatography and mass spectrometry. Peptides were subjected to exhaustive cleavage by the NS2B-NS3pro constructs (29). Intact peptides and C-terminal cleavage products were quantitatively removed from the digest by using magnetic beads coated with streptavidin (Seradyn, Indianapolis, IN) and a magnetic particle concentrator, Dynal MPC-96S (Invitrogen). The fluorescence of the N-terminal FAM-tagged cleavage products that were present in the supernatant was measured at an excitation wavelength of 492 nm and emission wavelength of 535 nm. The efficiency of the peptide cleavage was expressed as a percentage of peptide cleaved in the digest reactions.

Mass spectrometry analyses of the digest peptides. Peptides (1 μg; ~60 μM) were incubated with NS2B-NS3pro constructs (0.7 μg, 1.25 μM) for 2 h at 37°C in 20 μl of 10 mM Tris-HCl buffer (pH 8.0) containing 20% glycerol. The mass of the intact and digested peptides was determined by matrix-assisted laser desorption ionization–time of flight mass spectrometry using an Autoflex II mass spectrometer (Brucker Daltonics, Bremen, Germany).

Proteinase assays with fluorogenic peptides. The assay for NS3pro cleavage was performed in 10 mM Tris-HCl buffer (pH 8.0) containing 20% glycerol and 0.005% Brij 35. The Pyr-RTKR-AMC substrate and enzyme concentrations, unless indicated otherwise, were 24 μM and 10 nM, respectively. The total assay volume was 0.1 ml. Initial reaction velocities were monitored continuously at an excitation wavelength of 360 nm and an emission wavelength of 460 nm on a Spectramax Gemini EM fluorescence spectrophotometer (Molecular Devices, Sunnyvale, CA). All assays were performed in triplicate in 96-well plates. The values of K_m and k_{cat} were derived from a double reciprocal plot of $1/V_0$ versus $1/[S]$, using a Lineweaver-Burke transformation as follows: $1/V_0 = K_m/V_{max} \times 1/[S] + 1/V_{max}$, where V_0 is the initial velocity of the substrate hydrolysis, $[S]$ is the substrate concentration, V_{max} is the maximum rate of hydrolysis, and K_m is the Michaelis-Menten constant. The concentration of active proteinase was measured by using a fluorescence assay by titration against a standard aprotinin solution of a known concentration.

Modeling of the mutant structure. The structure of the WNV NS2B-NS3pro/aprotinin complex (PDB 2IJO) was used to model the structure of the R76L, P131K-T132P, and T52V mutants. The mutant residues were built by using PyMOL (8). Energy minimization was done by using PyMOL and CNS (3). Conformations of the mutant residues were identical to those in the ligand-free structure of DV NS2B-NS3pro (PDB 2FOM) (10).

RESULTS

Design, isolation, and cleavage kinetics of the mutant NS2B-NS3 constructs. NS3pro from DV and WNV share a 50% sequence identity. Despite the limited number of amino acid substitutions proximal to the catalytic triad, the two proteinases display significant differences in their substrate cleavage preferences (29). Active-site differences exist at Thr^{52}, Arg^{76}, and $Pro^{131}Thr^{132}$ (WNV sequence) (Fig. 1). Because these residues are located in the proximity of the protease catalytic triad, they have been selected for mutagenesis. Additional differences exist between the WNV and the DV NS3pro sequences, including S60, C78, P82, and V106 (WNV sequence). These residues, however, are distant from the NS3pro active site, and because of this structural relationship they have not been selected for our mutagenesis studies.

To explore the role of the Thr^{52}, Arg^{76}, and $Pro^{131}Thr^{132}$ residues in defining substrate preferences, we constructed chimeric proteins with single or double substitutions of DV residues into the WNV protein: the mutants were T52V, R76L, and P131K-T132P. Wild-type DV and WNV NS2B-NS3pro, together with the WNV/DV chimeras, were expressed in *E. coli* with C-terminal His tags and isolated from the soluble fraction by metal-chelating chromatography. In the course of purification, the 36-kDa NS2B-NS3 construct autocleaved the linker sequence, generating the noncovalently bound NS2B-NS3pro complex (29) (Fig. 2). Inhibitors of NS3pro activity completely inhibited autolysis of the wild-type and chimeric NS2B-NS3 constructs. Likewise, NS2B-NS3pro containing a catalytically inert active-site mutant (H51A) within NS3 was not autocleaved (29).

We next measured kinetic parameters and cleavage preferences for the wild-type and mutant proteins. Wild-type WNV was highly efficient in cleaving a Pyr-RTKR-AMC substrate. The T52V mutant exhibited a significant loss of k_{cat} that was, however, compensated for by an improvement in substrate binding, by a K_m value, which jointly produced a k_{cat}/K_m parameter that was similar to the wild-type WNV NS2B-NS3pro (Table 1). A similar decrease in k_{cat} for the P131K-T132P mutant was also partially compensated for by an improvement in the substrate binding, which resulted in a k_{cat}/K_m value that was similar to that of the wild-type DV proteinase. The kinetic parameters of the R76L mutant were similar to those of the wild-type WNV NS2B-NS3pro.

Peptide cleavage screens. To gain further insight into the subsite preferences of the DV and WNV proteinases, we designed libraries of synthetic nonapeptide substrates with the general Gly-Leu-Lys-Arg-P1′-P2′-Ala-Lys-Gly structure with systematic variations of the sequences around the scissile bond. To facilitate the follow-on cleavage screening assay, the N terminus and the constant C-terminal Gly of the peptides were tagged with a fluorescent tag and with a biotin tag, respectively. To screen the peptides, we selected exhaustive proteolysis conditions (an enzyme/substrate ratio of 1:50 to 51:150). We chose the $G^{2522}LKR \downarrow GGAK^{2529}$ peptide from the NS4B/NS5 WNV junction region for our current studies. According to our earlier study (29), this peptide, in contrast to many other peptide sequences, was cleaved with similar efficiency by the DV and WNV proteinases (72 and 73%, respectively). Peptides with a similar sequence, including GIKRGETD, LQKRGIVE,

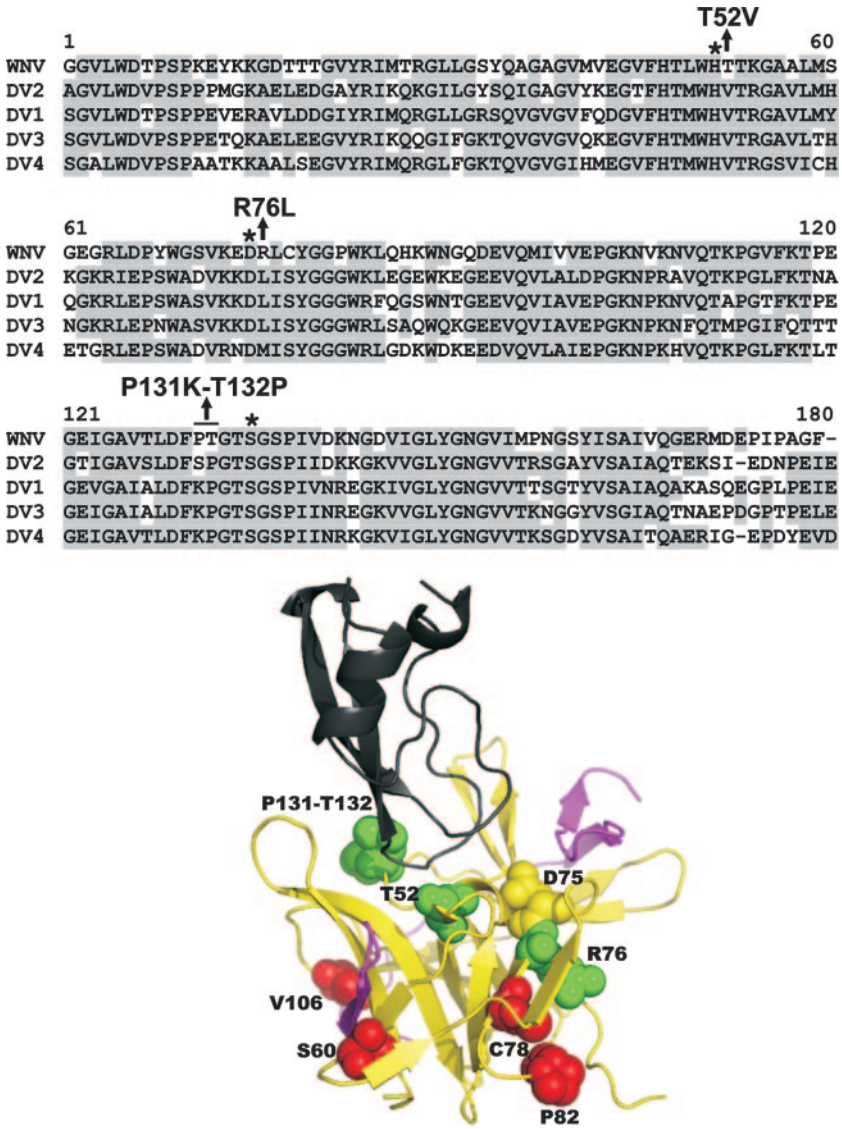

FIG. 1. Sequence alignment of the NS3pro sequence of WNV and DV serotypes 1 to 4 and the structure of the WNV NS2B-NS3pro. (Top) Homologous amino acid residue positions are shaded. The stars indicate the His[51], Asp[75], and Ser[135] of the catalytic triad. The arrows indicate the Thr→Val (T52V), Arg→Leu (R76L), and ProThr→LysPro (P131K-T132P) mutations in the WNV sequence. (Bottom) WNV NS2B-NS3pro (NS2B, magenta; NS3pro, yellow) with the bound inhibitor aprotinin (black). The mutated residues are shown in green. The additional residues, which distinguish WNV NS2B-NS3pro from DV NS2B-NS3pro, are in red. These residues have not been selected for mutagenesis because they are distant from the NS3pro active site (Asp[75] of the catalytic triad is shown in yellow).

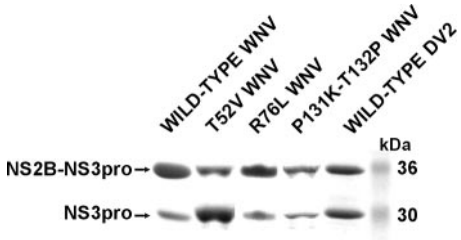

FIG. 2. Purified DV and WNV NS2B-NS3pro constructs. The wild-type DV and WNV NS2B-NS3pro, as well as the T52V, R76L, and P131K-T132P mutants of the WNV NS3pro, were C terminally tagged with a His_6 tag and then expressed in *E. coli.* Each of the constructs was purified from the soluble fraction of *E. coli* lysate and analyzed by sodium dodecyl sulfate-polyacrylamide gel electrophoresis, followed by Coomassie staining.

LSKRQHPG, LVTAGHGQ, and MLKKGMTT, were completely resistant to proteolysis by both proteinases. On the other hand, the peptides KKQRAGVL, LYKRYGGF, MLK RGMPR, and NQKRYGGF were resistant to WNV proteinase but were cleaved by DV proteinase with 11, 48, 49, and 7% efficiency, respectively. The reliability of the synthesis and the accuracy of the assay were further confirmed by the analysis of triplicate and duplicate samples of the multiple peptides. For example, WNV NS2B-NS3pro proteolysis of two batches of the peptide NRKR ↓ GGPA resulted in 78 and 77% cleavage. Cleavage of the peptide QRRR ↓ GGTA by WNV NS2B-NS3pro twice resulted in a 58% cleavage. Three individual batches of the peptide AQRR ↓ GRIG resulted in 3, 2, and 0% cleavages by WNV NS2B-NS3pro. Similarly, DV NS2B-NS3pro generated 45,

TABLE 1. Cleavage of fluorescent peptide substrate Pyr-RTKR-AMC by DV and WNV constructs

NS2B-NS3pro type	Mean ± SD		
	K_m (μM)	k_{cat} (s^{-1})	k_{cat}/K_m ($mM^{-1}\ s^{-1}$)
WNV wild type	71 ± 15	6.3 ± 0.35	88 ± 12
WNV R76L	89 ± 16	7.3 ± 0.4	82 ± 11
WNV T52V	0.13 ± 0.006	0.013 ± 0.0006	100 ± 10
WNV P131K-T132P	0.13 ± 0.006	0.002 ± 0.0001	16 ± 2
DV2 wild type	3.6 ± 0.2	0.02 ± 0.001	5.5 ± 0.5

37, and 36% cleavages of three batches of the peptide AQRR ↓ GRIG. These results emphasize the high reliability and consistency of our screening approach.

The G^{2522}LKRGGAK^{2529} peptide was assayed in a positional scanning format where the P4-P1 and the P3′-P4′ positions were fixed and the P1′ and P2′ positions were each randomized with 17 and 14 amino acids (Fig. 3; the "X" represents the randomized positions). Because the library was tested at highly similar peptide substrate concentrations under exhaustive proteolysis conditions, the relative significance of the amino acid substitutions could be directly measured. Consistent with our earlier studies (29), a significant selectivity for Gly at both the P1′ and the P2′ positions was observed with the wild-type WNV enzyme. In contrast, the DV NS2B-NS3pro tolerated well the presence of many amino acid types, except for negatively charged Asp and Glu, at either the P1′or the P2′ positions. These screens demonstrated that the R76L and P131K-T132P mutations shifted substrate cleavage preference of the WNV protease toward those of the DV enzyme, whereas the effect of the T52V WNV mutation was insignificant.

To confirm further that R76L and P131K-T132P mutations shifted the specificity of the WNV proteinase to that of the DV enzyme and to observe whether the mutants complied with the specificity of the DV enzyme in cleaving a wide variety of the peptide sequences, we used additional variants of the GLKR ↓ GGAK sequence. We tested the following variants: GLKR ↓ AAAK, GLKR ↓ VVAK, GLKR ↓ LLAK, GLKR ↓ IIAK, GLKR ↓ FFAK, GLKR ↓ WWAK, GLKR ↓ MMAK, GLKR ↓ SSAK, GLKR ↓ PPAK, GLKR ↓ TTAK, GLKR ↓ YYAK, GLKR ↓ NNAK, GLKR ↓ QQAK, GLKR ↓ EEAK, and GLKR ↓ HHAK, which had the same residue at both P1′ and P2′. In addition, we evaluated the peptide GLKR ↓ TSAK because the related GLKR ↓ TGAK and GLKR ↓ GSAK peptides were efficiently cleaved by DV NS2B-NS3pro (77 and 82%, respectively; Fig. 3) but poorly by the WNV enzyme (2 and 9%, respectively; Fig. 3).

Because Gly-Gly was not present at P1′-P2′, WNV NS2B-NS3pro was incapable of cleaving these peptides (Fig. 4). In contrast, DV proteinase cleaved them efficiently. The sequences with hydrophobic amino acid residues at P1′ and P2′, including Phe-Phe, Ile-Ile, Leu-Leu, and Val-Val but not Trp-Trp, were most sensitive to the DV proteolysis. The cleavage profile of the WNV T52V mutant was obviously distinct from that of the DV proteinase. Compared to the WNV proteinase, this mutant acquired the ability to hydrolyze peptides with either Gln-Gln, Asn-Asn or His-His at P1′ and P2′. The R76L and, especially, the P131K-T132P WNV chimera performed in these cleavage tests similarly to the DV proteinase.

To additionally corroborate the shift in the cleavage preferences of the R76L and P131K-T132 mutants, we measured the cleavage of the K^{97}RKK ↓ TSLC^{104} peptide in the cleavage reactions using the WNV and DV constructs. This peptide was derived from the cleavage site of the capsid protein C of DV type 3 (Table 2). According to our results, the cleavage efficiencies of this peptide by the wild type, T52V, R76L, and P131K-T132P WNV constructs and DV NS2B-NS3pro were 8, 1, 80, 62, and 47%, respectively. These data support the shift of the cleavage preferences for both of the R76L and P131K-T132P WNV constructs toward that of the DV proteinase.

Overall, it appears that the T52V mutation did not cause any significant differences in the cleavage subsite specificity of the construct and, as a result, the cleavage preferences of the T52V mutant construct were similar to those of the original WNV proteinase. In contrast, the R76L mutation modified the substrate cleavage specificity of the WNV construct, making its cleavage preferences similar to those of the DV proteinase. The P131K-T132P mutant cleavage preferences were also significantly modified toward the DV proteinase.

Mass spectrometric analysis of the peptides. To corroborate our findings, we used proteolysis of the GLKR ↓ FGAK peptide, followed by mass spectrometry analyses of the digest products. In this case, the GLKR ↓ FGAK peptide was not tagged, and it was synthesized without the C-terminal Gly. The GLKR ↓ FGAK peptide, because of the presence of the bulky hydrophobic Phe at P1′, was highly resistant to the wild-type WNV proteinase and, in contrast, was sensitive to the DV enzyme. In agreement with the data from the peptide cleavage screen, the mass spectrometry analysis confirmed that the GLKR ↓ FGAK 858-Da peptide was resistant to proteolysis by the wild-type and T52V WNV proteins (Fig. 5). In turn, the peptide was readily digested by the R76L WNV and P131K-T132P mutants and the DV NS2B-NS3pro and generated the expected 455-Da GLKR digest product (Fig. 5).

Natural cleavage sites in the flavivirus polyprotein precursor. The NS3 proteinase is essential for the cleavage of six distinct sequences in the polyprotein (Table 2). Consistent with its furin-like, restricted, substrate cleavage specificity (20, 28, 30, 36), NS3pro requires the presence of positively charged Arg and either Arg or Lys at the P1 and P2 positions, respectively, for efficient cleavage of the scissile bond. These requirements result in the conservation of natural cleavage sites in the flavivirus polyprotein precursor. The only exception is the cleavage site at the NS2B-NS3 boundary, at which Gln occupies the P2 position in all four DV serotypes. In the polyprotein precursor, the dibasic (Lys/Arg)-Arg motif is followed by a small or polar residue including predominantly Gly and Ser. In the WNV polyprotein Gly most frequently occupies both the P1′ and the P2′ positions. A similar pattern is also characteristic for Japanese encephalitis virus. In turn, in yellow fever virus and in all four DV serotypes, Ser, or sometimes Ala or Thr, is at the P1′ site. When Ser, Ala, or Thr occupies P1′ position, multiple amino acid types (Ser, Thr, Ala, Val, Leu, Ile, and Trp) are allowed at the P2′ position in DV. As long as Gly occupies P1′ (at the NS4B-NS5 boundary) and P2′ (at the NS2B-NS3 boundary) in DV, the other P′ position may be occupied by Ser, Ala, or Thr. This specificity pattern correlates

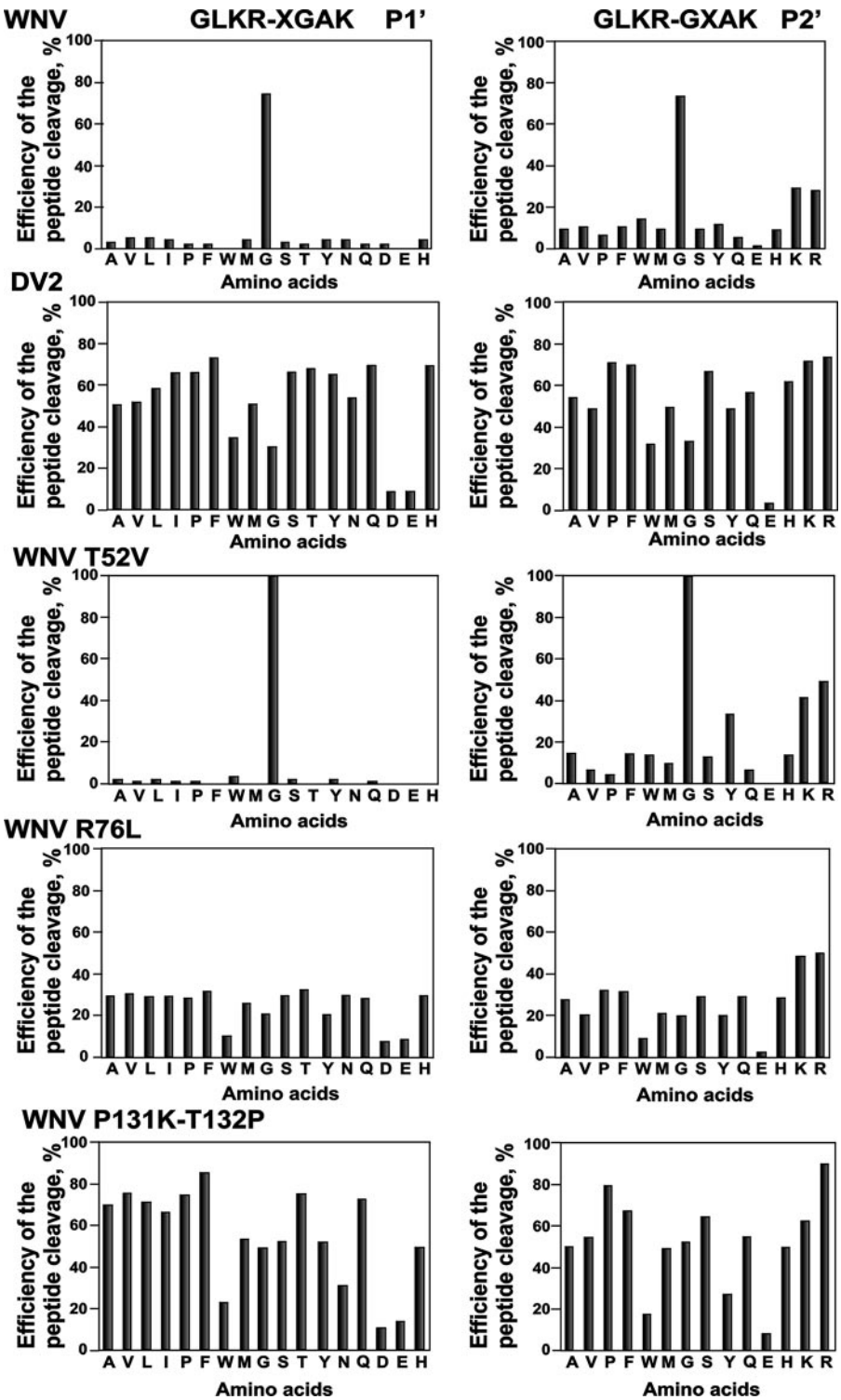

FIG. 3. P1′-P2′ subsite substrate specificity of the wild-type DV type 2 NS2B-NS3pro and the wild-type and mutant (T52V, R76L, and P131-T132P) NS2B-NS3pro of WNV. The P4-P1 and the P3′-P4′ positions of the GLKR ↓ GGAK peptide were fixed, and the P1′ and P2′ positions were each randomized with 17 and 14 amino acids, respectively. X represents the randomized positions. The NS2B-NS3pro was added to the individual peptides in the wells of a 96-well plate, and the samples were processed as described in Materials and Methods. Note the strong preference of the WNV enzyme for the Gly at the P1′ and P2′ positions and the DV-like specificity of the R76L and P131K-T132P mutants.

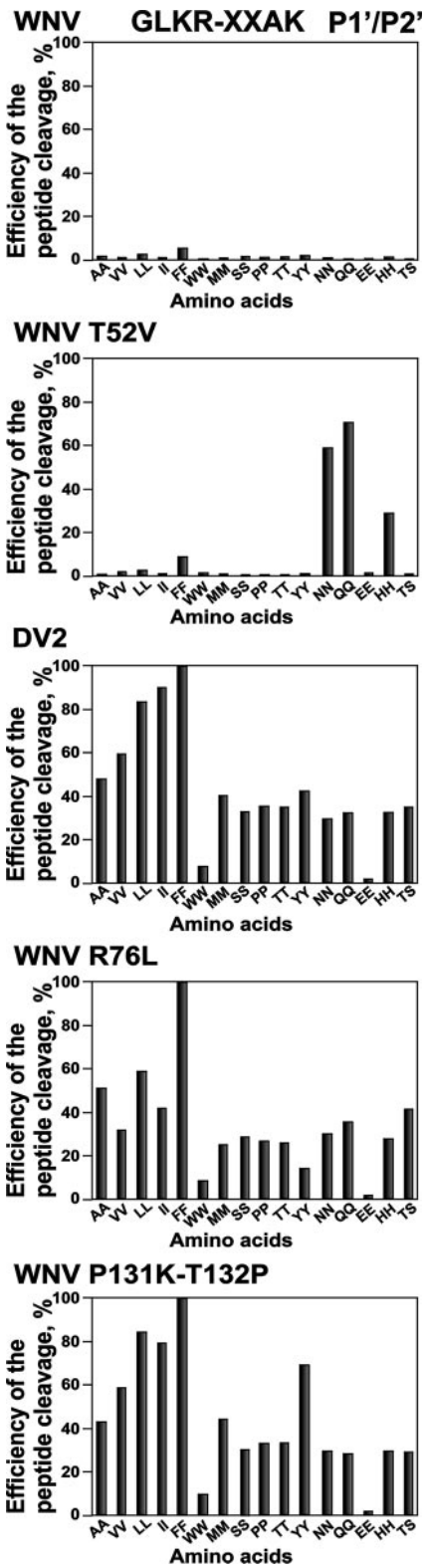

FIG. 4. P1′-P2′ subsite specificity of the mutant WNV constructs. The P4-P1 and the P3′-P4′ positions of the GLKR ↓ GGAK peptide were fixed, and the P1′ and P2′ positions were each substituted with a pair of identical residues. The proteinase was added to the individual peptides in the wells of a 96-well plate, and the samples were processed as described in Materials and Methods. Note the striking similarity between the wild-type DV NS2B-NS3pro and the WNV P131-T132P mutant.

well with the results of the peptide cleavage screens and indicates that WNV NS3pro specifically developed a capability for cleaving the Gly-Gly motifs, while the DV enzyme adopted a less restricted specificity to process the natural cleavage sites in the polyprotein precursor. This statement, however, does not exclude the possibility that the cleavage sites may have evolved to adjust the preferences of the proteinase or, most probably, the two evolved together.

DISCUSSION

Because of its essential function in posttranslational processing of the viral polyprotein precursor, the NS3 serine proteinase is a promising target for antiflavivirus drugs (32). The design of effective inhibitors is exceedingly difficult if the structural and functional parameters of flavivirus proteinases are not precisely determined. Recently, we and others determined the crystal structure of the two-component NS2B-NS3pro complex from DV and WNV (1, 10). There are approximately 50 nonidentical residue positions in the 180-residue WNV NS3pro compared to that of DV NS3pro. Our expectations, based on the crystal structure of WNV NS2B-NS3pro, were that neither S60, C78, P82, nor V106 would have a pronounced effect on substrate binding or enzyme activity, whereas R76, P131-T132, and T52 are likely to be involved in defining the cleavage preferences of the flavivirus proteases (Fig. 1). Additional structural analysis of the DV and the WNV NS2B-NS3pro suggests that neither Thr^{52} in WNV nor Val^{52} in DV, despite their proximity to the catalytic triad His^{51}, would have a pronounced effect on substrate binding or enzyme activity (Fig. 6). We expected that the R76L mutant would affect the substrate binding pocket and the catalytic potency of the WNV NS3pro and that this effect would result in promiscuous activity of the R76L WNV mutant. Based on the structural parameters of the DV and WNV NS2B-NS3pro, we also expected that the Pro^{131}-Thr^{132} motif in WNV, which corresponds to the Lys^{131}-Pro^{132} sequence in DV types 1, 3, and 4, would play a significant role in defining the P1′/P2′ subsite specificity of NS2B-NS3pro (Fig. 6). These considerations served as the structural rationale for our mutagenesis studies.

We used site-directed mutagenesis to incorporate DV residues into the sequence of WNV NS3pro. The chimeras were expressed in *E. coli* cells and then purified and assayed in a P1′-P2′ positional scanning format against the peptide library based on the G^{2522}LKR ↓ GGAK^{2529} peptide from the NS4B/NS5 WNV junction. The peptide cleavage data confirmed our hypothesis and demonstrated that the cleavage preferences were basically unchanged in the T52V mutant, whereas the R76L and, especially, the P131K-T132P mutations largely transformed the cleavage preferences of the WNV NS3pro into those of DV. The kinetic parameters of the WNV NS3pro mutants against the fluorescence substrate Pyr-RTKR-AMC were also consistent with the results of the peptide screening and structural analysis.

The crystal structure of the WNV NS2B-NS3pro-aprotinin complex (PDB 2IJO) that we recently determined at a 2.3-Å resolution (1) shows that His^{51}, Thr^{52}, and Ala^{36} form the S1′ site (Fig. 6A). As a result, the cavity that represents the S1′ site is small. The S1′ cavity of the WNV proteinase suggests that its size is sufficient for binding small residues including Gly, Ala,

TABLE 2. Sequence of natural cleavage sites of NS3 proteinase in capsid protein C and at the NS2A/NS2B, NS2B/NS3, NS3/NS4A, NS4A/NS4B, and NS4B/NS5 boundaries of the polyprotein precursor[a]

Virus	Sequence				
	Capsid C	NS2A/NS2B	NS2B-NS3	NS3/NS4A	NS4B/NS5
WNV	Q^{101}KKR↓**GG**TA^{108}	N^{1367}RKR↓**G**WPA^{1374}	Y^{1498}TKR↓**GG**VL^{1505}	S^{2117}GKR↓SQIG^{2124}	G^{2522}LKR↓**GG**AK^{2529}
JEV	Q^{102}NKR↓**GG**NE^{109}	N^{1370}KKR↓**G**WPA^{1377}	T^{1501}TKR↓**GG**VF^{1508}	A^{2120}GKR↓SAVS^{2127}	S^{2564}LKR↓**G**RPG^{2571}
YFV	R^{98}KRR↓SHDV^{105}	F^{1351}GRR↓SIPV^{1358}	G^{1481}ARR↓S**G**DV^{1488}	E^{2104}GRR↓**G**AAE^{2111}	T^{2503}GRR↓**G**SAN^{2510}
DV1	R^{97}RKR↓SVTM^{104}	W^{1341}GRK↓SWPL^{1348}	K^{1471}KQR↓S**G**VL^{1478}	A^{2090}GRR↓SVSG^{2097}	G^{2489}GRR↓**G**TGA^{2496}
DV2	R^{97}RRR↓TAGV^{104}	S^{1342}KKR↓SWPL^{1349}	K^{1472}KQR↓A**G**VL^{1479}	A^{2090}GRK↓SLTL^{2097}	N^{2488}TRR↓**G**TGN^{2495}
DV3	K^{97}RKK↓TSLC^{104}	L^{1340}KRR↓SWPL^{1347}	Q^{1470}TQR↓S**G**VL^{1477}	A^{2089}GRK↓SIAL^{2096}	T^{2487}GKR↓**G**TGS^{2494}
DV4	G^{96}RKR↓STIT^{103}	A^{1341}SRR↓SWPL^{1348}	K^{1471}TQR↓S**G**AL^{1478}	S^{2089}GRK↓SITL^{2096}	T^{2484}PRR↓**G**TGT^{2491}

[a] WNV, West Nile virus; JEV, Japanese encephalitis virus; YFV, yellow fever virus; DV1 to -4, dengue virus serotypes 1 to 4, respectively. The P1′/P2′ Gly is indicated in boldface.

Ser, and Thr. In addition, Thr^{132} in WNV NS3pro forms a hydrogen bond with the peptide bond involving the P1′ residue. This bond is unique for WNV because in the DV NS3 polypeptide chain the Pro^{132} residue that occupies this position is incapable of making a similar hydrogen bond. According to our modeling data, the hydrogen bond involving Thr^{132} stabilizes the backbone conformations of the P1′ and P2′ residues, allowing their side chains to make tight contacts with His^{51} and Thr^{132} of WNV NS3pro. These events limit the mobility of the P2′ residues, thus leading to the preferred Gly at the P2′ position. This does not affect the P1′-P2′ interactions because the side chain of Lys^{131} is exposed to a solvent and can adopt multiple conformations without affecting the S2′ site.

Structural modeling also explains well the effect of the R76L mutation (Fig. 6C). Thus, in contrast to Arg^{76}, the hydrophobic side chain of Leu^{76} cannot fit well into a limited size cavity. As a result, Leu^{76} interferes with the structure of the neighboring Trp^{83} and Val^{166}. Energy minimization of the R76L mutant structure suggests that the loop including Asp^{75} is likely to shift away, affecting the position and the interactions of the active site His^{51} side with the P1-P2′ subsites. Modeling of the T52V mutant predicts that there will be no effect by this mutation on substrate binding parameters (Fig. 6B). Our positional scanning studies support this suggestion.

Recently, we determined the structure of the WNV NS2B-NS3 in complex with the trypsin inhibitor, aprotinin (1). While our study was in progress, the structures of the two-component WNV and DV NS2B-NS3pro in complex with the substrate-based inhibitor benzoyl-norleucine (P4)-lysine (P3)-arginine (P2)-arginine (P1)-aldehyde (Bz-Nle-Lys-Arg-Arg-H) became available (10). A direct comparison of the available structures failed to produce an unambiguous structural rationale for the distinct P1′-P2′ subsite specificity of the WNV and the DV proteinases. We, however, determined that aprotinin binding stimulated, by an "induced fit" mechanism (15), a catalytically competent conformation of the "oxyanion hole" in the proteinase domain. This hole, lined by main chain nitrogens (from Gly^{133}-Ser^{135} in WNV) is misformed in the peptide-based inhibitor-bound structure of DV NS2B-NS3pro (10), because the peptide bond between Thr^{132} and Gly^{133} is flipped. As a result, the flipped bond creates an α-helical conformation for residues 131 to 135 that is stabilized by two hydrogen bonds that are absent in the productive conformation. Thus, our structural data suggest that the productive conformation of the oxyanion

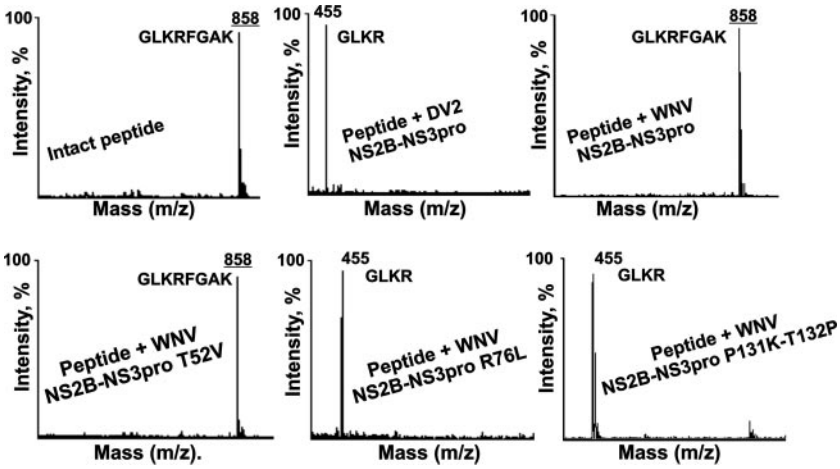

FIG. 5. Mass spectrometric analysis of the GLKR ↓ FGAK peptide cleavage products. The peptide was subjected to proteolysis by wild-type NS2B-NS3pro from DV and WNV and by the T52V, R76L, and P131K-T132P mutants. The mass of the digest products was then determined by matrix-assisted laser desorption ionization–time of flight mass spectrometry. The molecular mass of the intact peptide (underlined) and the cleavage product are shown on the panels. There was no difference between the calculated and the estimated masses of the peptides. Note that, because of the presence of Phe in the P1′ position, both the wild-type and the T52V mutant were incapable of cleaving the GLKR ↓ FGAK peptide that, in turn, was efficiently digested by the DV proteinase and the R76L and the P131KT132P WNV mutants.

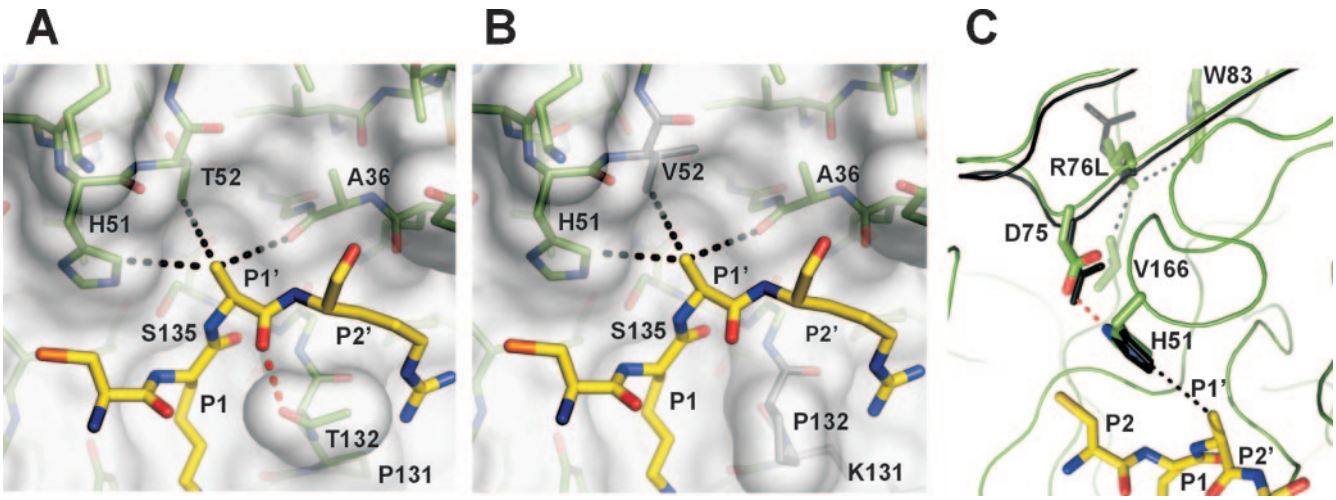

FIG. 6. Structural modeling of the NS2B-NS3pro specificity. (A) Active site of the wild-type WNV NS2B-NS3pro (green) with selected aprotinin residues (yellow) (PDB 2IJO). (B) Model of WNV NS2B-NS3pro with the T52V and P131K-T132P substitutions. (C) Model of the WNV NS2B-NS3pro R76L mutant. The black and green solid lines indicate the protein backbone and the selected side chains in the wild-type and the mutant enzyme, respectively. The black and red dotted lines indicate hydrogen bonds that are affected by the R76L mutation.

hole of WNV NS2B-NS3pro is acquired only in the presence of a substrate with an appropriate P1′ residue. We suspect that a similar "induced fit" mechanism leads to the productive conformation of the active site oxyanion hole of the DV proteinase, thus widening the P1′-P2′ subsites, which can accommodate, as a result, the bulky hydrophobic residues including Phe, Val, Ile, and Leu (but not Trp). It is tempting to hypothesize that the presence of the excessive size Trp at both P1′-P2′ sites interferes with the productive positioning of the peptide in the active site of the DV proteinase and, as a result, the G^{2522}LKRWWAK^{2529} peptide was resistant to the proteolysis. Similar considerations are applicable for the G^{2522}LK REEAK^{2529} peptide in which the presence of Glu at both P1′ and P2′ sites seems to interfere with the productive orientation of the peptide in the active site groove. On the other hand, the available crystal structures do not allow us to draw an unambiguous structural rationale regarding the enhanced ability of the T52V WNV mutant against the peptides with either Gln or Asn at both P1′ and P2′ positions.

Our results support and extend the previous findings of several groups (6, 7, 10, 19, 20, 23, 24, 26, 36) and also provide a structural rationale for the reduced selectivity of the DV proteinase, which tolerates well the presence of a number of amino acid residue types at both P1′ and P2′ positions. Importantly, earlier studies did not determine any significant difference in the P1′ or P2′ specificity between the WNV and DV enzymes (6, 7, 20). Based on the significant levels of homology within the NS3pro flavivirus sequences, it was expected that an inhibitor designed against one protease would be equally potent against multiple flaviviruses, thus acting as a "pan-inhibitor." Based on our data, it is likely that a pan-inhibitor should target the P1- and P1-binding subsites, whereas the specific inhibitors would, most probably, target the divergent P1′ and P2′ subsites of the flavivirus NS3pro. It also appears that the most sensitive and selective peptide substrates of flavivirus NS2B-NS3pro will not necessary recapitulate the natural cleavage motifs. The cleavage substrate sequences we identified will be useful in high-throughput screenings for DV NS2B-NS3 inhibitors.

Overall, our results validate the structural parameters of the NS2B-NS3pro and prove that the available structural coordinates may be used as a template for drug design. Our findings represent the first instance of engineering a viral proteinase with switched substrate cleavage preferences and should support the redesign of other proteinases. We hope that the data presented here will refocus rational drug design and facilitate the development of novel and effective, substrate-based inhibitors of the flavivirus proteinases.

ACKNOWLEDGMENTS

This study was supported by National Institutes of Health grants AI056385, AI061139, and RR020843 (A.Y.S.).

REFERENCES

1. **Aleshin, A. E., S. A. Shiryaev, A. Y. Strongin, and R. C. Liddington.** Structural evidence for multiple levels of regulation of flaviviral protease activity. Protein Sci., in press.
2. **Beasley, D. W.** 2005. Recent advances in the molecular biology of West Nile virus. Curr. Mol. Med. **5:**835–850.
3. **Brunger, A. T., P. D. Adams, and L. M. Rice.** 1997. New applications of simulated annealing in X-ray crystallography and solution NMR. Structure **5:**325–336.
4. **Cahour, A., B. Falgout, and C. J. Lai.** 1992. Cleavage of the dengue virus polyprotein at the NS3/NS4A and NS4B/NS5 junctions is mediated by viral protease NS2B-NS3, whereas NS4A/NS4B may be processed by a cellular protease. J. Virol. **66:**1535–1542.
5. **Chambers, T. J., D. A. Droll, Y. Tang, Y. Liang, V. K. Ganesh, K. H. Murthy, and M. Nickells.** 2005. Yellow fever virus NS2B-NS3 protease: characterization of charged-to-alanine mutant and revertant viruses and analysis of polyprotein-cleavage activities. J. Gen. Virol. **86:**1403–1413.
6. **Chappell, K. J., T. A. Nall, M. J. Stoermer, N. X. Fang, J. D. Tyndall, D. P. Fairlie, and P. R. Young.** 2005. Site-directed mutagenesis and kinetic studies of the West Nile virus NS3 protease identify key enzyme-substrate interactions. J. Biol. Chem. **280:**2896–2903.
7. **Chappell, K. J., M. J. Stoermer, D. P. Fairlie, and P. R. Young.** 2006. Insights to substrate binding and processing by West Nile virus NS3 protease through combined modeling, protease mutagenesis, and kinetic studies. J. Biol. Chem. **281:**38448–38458.
8. **DeLano, W. L.** 2002. The PyMOL user's manual. DeLano Scientific, San Carlos, CA.
9. **Droll, D. A., H. M. Krishna Murthy, and T. J. Chambers.** 2000. Yellow fever

virus NS2B-NS3 protease: charged-to-alanine mutagenesis and deletion analysis define regions important for protease complex formation and function. Virology **275:**335–347.

10. **Erbel, P., N. Schiering, A. D'Arcy, M. Renatus, M. Kroemer, S. P. Lim, Z. Yin, T. H. Keller, S. G. Vasudevan, and U. Hommel.** 2006. Structural basis for the activation of flaviviral NS3 proteases from dengue and West Nile virus. Nat. Struct. Mol. Biol. **13:**372–373.
11. **Falgout, B., R. H. Miller, and C. J. Lai.** 1993. Deletion analysis of dengue virus type 4 nonstructural protein NS2B: identification of a domain required for NS2B-NS3 protease activity. J. Virol. **67:**2034–2042.
12. **Falgout, B., M. Pethel, Y. M. Zhang, and C. J. Lai.** 1991. Both nonstructural proteins NS2B and NS3 are required for the proteolytic processing of dengue virus nonstructural proteins. J. Virol. **65:**2467–2475.
13. **Gubler, D. J.** 1998. Dengue and dengue hemorrhagic fever. Clin. Microbiol. Rev. **11:**480–496.
14. **Hachmann, J., and M. Lebl.** 2006. Search for optimal coupling reagent in multiple peptide synthesizer. Biopolymers **84:**340–347.
15. **Koshland, D. E.** 1958. Application of a theory of enzyme specificity to protein synthesis. Proc. Natl. Acad. Sci. USA **44:**98–104.
16. **Kozlov, I. A., P. C. Melnyk, C. Zhao, J. P. Hachmann, V. Shevchenko, A. Srinivasan, D. L. Barker, and M. Lebl.** 2006. A method for rapid protease substrate evaluation and optimization. Comb. Chem. High Throughput Screen. **9:**481–487.
17. **Lebl, M.** 1999. New technique for high-throughput synthesis. Bioorg. Med. Chem. Lett. **9:**1305–1310.
18. **Lebl, M., and J. Hachmann.** 2005. High-throughput peptide synthesis. Methods Mol. Biol. **298:**167–194.
19. **Leung, D., K. Schroder, H. White, N. X. Fang, M. J. Stoermer, G. Abbenante, J. L. Martin, P. R. Young, and D. P. Fairlie.** 2001. Activity of recombinant dengue 2 virus NS3 protease in the presence of a truncated NS2B cofactor, small peptide substrates, and inhibitors. J. Biol. Chem. **276:**45762–45771.
20. **Li, J., S. P. Lim, D. Beer, V. Patel, D. Wen, C. Tumanut, D. C. Tully, J. A. Williams, J. Jiricek, J. P. Priestle, J. L. Harris, and S. G. Vasudevan.** 2005. Functional profiling of recombinant NS3 proteases from all four serotypes of dengue virus using tetrapeptide and octapeptide substrate libraries. J. Biol. Chem. **280:**28766–28774.
21. **Mukhopadhyay, S., R. J. Kuhn, and M. G. Rossmann.** 2005. A structural perspective of the flavivirus life cycle. Nat. Rev. Microbiol. **3:**13–22.
22. **Murthy, H. M., S. Clum, and R. Padmanabhan.** 1999. Dengue virus NS3 serine protease: crystal structure and insights into interaction of the active site with substrates by molecular modeling and structural analysis of mutational effects. J. Biol. Chem. **274:**5573–5580.
23. **Murthy, H. M., K. Judge, L. DeLucas, and R. Padmanabhan.** 2000. Crystal structure of Dengue virus NS3 protease in complex with a Bowman-Birk inhibitor: implications for flaviviral polyprotein processing and drug design. J. Mol. Biol. **301:**759–767.
24. **Nall, T. A., K. J. Chappell, M. J. Stoermer, N. X. Fang, J. D. Tyndall, P. R. Young, and D. P. Fairlie.** 2004. Enzymatic characterization and homology model of a catalytically active recombinant West Nile virus NS3 protease. J. Biol. Chem. **279:**48535–48542.
25. **Niyomrattanakit, P., P. Winoyanuwattikun, S. Chanprapaph, C. Angsuthanasombat, S. Panyim, and G. Katzenmeier.** 2004. Identification of residues in the dengue virus type 2 NS2B cofactor that are critical for NS3 protease activation. J. Virol. **78:**13708–13716.
26. **Niyomrattanakit, P., S. Yahorava, I. Mutule, F. Mutulis, R. Petrovska, P. Prusis, G. Katzenmeier, and J. E. Wikberg.** 2006. Probing the substrate specificity of the dengue virus type 2 NS3 serine protease by using internally quenched fluorescent peptides. Biochem. J. **397:**203–211.
27. **Samuel, C. E.** 2002. Host genetic variability and West Nile virus susceptibility. Proc. Natl. Acad. Sci. USA **99:**11555–11557.
28. **Seidah, N. G.** 2006. Unexpected similarity between the cytosolic West Nile virus NS3 and the secretory furin-like serine proteinases. Biochem. J. **393:** e1–e3.
29. **Shiryaev, S. A., I. A. Kozlov, B. I. Ratnikov, J. W. Smith, M. Lebl, and A. Y. Strongin.** 2006. Cleavage preference distinguishes the two-component NS2B-NS3 serine proteinases of dengue and West Nile viruses. Biochem. J. **401:**743–752.
30. **Shiryaev, S. A., B. I. Ratnikov, A. V. Chekanov, S. Sikora, D. V. Rozanov, A. Godzik, J. Wang, J. W. Smith, Z. Huang, I. Lindberg, M. A. Samuel, M. S. Diamond, and A. Y. Strongin.** 2006. Cleavage targets and the D-arginine-based inhibitors of the West Nile virus NS3 processing proteinase. Biochem. J. **393:**503–511.
31. **Thomas, G.** 2002. Furin at the cutting edge: from protein traffic to embryogenesis and disease. Nat. Rev. Mol. Cell. Biol. **3:**753–766.
32. **van der Meulen, K. M., M. B. Pensaert, and H. J. Nauwynck.** 2005. West Nile virus in the vertebrate world. Arch. Virol. **150:**637–657.
33. **Xu, T., A. Sampath, A. Chao, D. Wen, M. Nanao, P. Chene, S. G. Vasudevan, and J. Lescar.** 2005. Structure of the dengue virus helicase/nucleoside triphosphatase catalytic domain at a resolution of 2.4 Å. J. Virol. **79:**10278–10288.
34. **Yamshchikov, V. F., D. W. Trent, and R. W. Compans.** 1997. Upregulation of signalase processing and induction of prM-E secretion by the flavivirus NS2B-NS3 protease: roles of protease components. J. Virol. **71:**4364–4371.
35. **Yon, C., T. Teramoto, N. Mueller, J. Phelan, V. K. Ganesh, K. H. Murthy, and R. Padmanabhan.** 2005. Modulation of the nucleoside triphosphatase/RNA helicase and 5′-RNA triphosphatase activities of dengue virus type 2 nonstructural protein 3 (NS3) by interaction with NS5, the RNA-dependent RNA polymerase. J. Biol. Chem. **280:**27412–27419.
36. **Yusof, R., S. Clum, M. Wetzel, H. M. Murthy, and R. Padmanabhan.** 2000. Purified NS2B/NS3 serine protease of dengue virus type 2 exhibits cofactor NS2B dependence for cleavage of substrates with dibasic amino acids in vitro. J. Biol. Chem. **275:**9963–9969.